land

MDPI

Article

Spatial and Temporal Variations of Habitat Quality and Influencing Factors in Urban Agglomerations on the North Slope of Tianshan Mountains, China

Ran Wang [1,†], Honglin Zhuang [1,†], Mingkai Cheng [1], Hui Yang [1,*], Wenfeng Wang [2,3], Hui Ci [1] and Zhaojin Yan [1]

[1] School of Resources and Geosciences, China University of Mining and Technology, Xuzhou 221116, China
[2] Key Laboratory of Coalbed Methane Resources and Reservoir Formation Process, Ministry of Education, School of Resource and Geoscience, China University of Mining and Technology, Xuzhou 221008, China
[3] School of Geology and Mining Engineering, Xinjiang University, Urumqi 830047, China
* Correspondence: yanghui@cumt.edu.cn
† These authors contributed equally to this work.

Abstract: The northern slope of the Tianshan Mountains city cluster (NSTM), as a key urban agglomeration for the development of western China, has experienced rapid regional economic development and high population concentration since the twenty-first century. Accompanied by the increase in human activities in the NSTM, it has significantly altered the land use structure, leading to varying levels of habitat disturbance and degradation. In this paper, based on the land use and land cover (LULC) of NSTM from 2000 to 2020. The InVEST model was employed to assess habitat quality, revealing notable spatial and temporal variations. A geoprobe was further employed to explore the key drivers of the spatially distributed pattern of habitat quality in the research region. The results show that (1) from 2000 to 2020, the NSTM was largely characterized by grassland, unused land, and cropland in terms of land use, with a notable expansion of cropland and construction land; (2) the overall habitat quality in the study area is poor, with a clear spatial distribution pattern of high in the south and low in the north, with a predominance of low grades, and a trend of decreasing and then increasing is shown in the temporal direction; (3) under the influence of rapid urbanization in the region, the degradation degree of habitat quality on the NSTM shows a distinct radial structure, with high degradation in the middle and low degradation at the edges, and shows the trend of "increase-decrease-increase" over time; and (4) the results of the geodetector show that altitude and land use type have the greatest influence on habitat quality on the NSTM, indicating that the habitat quality of the research region is primarily influenced by the type of land use.

Keywords: northern slopes of Tianshan Mountain city cluster; land use; InVEST model; habitat quality; influencing factors

Received: 22 January 2025
Revised: 20 February 2025
Accepted: 3 March 2025
Published: 5 March 2025

Citation: Wang, R.; Zhuang, H.; Cheng, M.; Yang, H.; Wang, W.; Ci, H.; Yan, Z. Spatial and Temporal Variations of Habitat Quality and Influencing Factors in Urban Agglomerations on the North Slope of Tianshan Mountains, China. *Land* **2025**, *14*, 539. https://doi.org/10.3390/land14030539

1. Introduction

In the light of global warming, the importance of habitat quality (HQ) as a core indicator for assessing ecosystem health and biodiversity has become increasingly prominent [1]. An essential measure of ecosystem services and ecosystem health, HQ shows how well organisms can live and reproduce in a particular ecological niche. Human activities, such as urbanization and economic growth, have made habitat shrinkage, ecological carrying capacity loss, and the fragmentation of arable land worse. HQ research has attracted

increasing attention, and examining the features of changes in HQ, revealing the factors affecting regional ecosystems, and predicting HQ have become research hotspots. Ecological survey techniques and evaluation model methods are the two categories of HQ research methodologies. The ecological survey approach gathers pertinent indicators for evaluating HQ throughout the investigated region via field surveys and employs them to establish a system of indicators for assessing HQ. This method is time-consuming and labor-intensive, making it more suitable for small-scale studies and challenging to carry out long time-series evolutionary studies [2]. In contrast, the quantitative evaluation modeling approach provides a quantitative assessment of habitat quality by means of mathematical models and remotely sensed data. This approach has the advantages of being efficient and cost-effective, allowing for the analysis of spatial and temporal dynamics. Therefore, many scholars have chosen to use quantitative evaluation models to carry out their research. Currently, commonly used models include the Habitat Suitability Index model (HSI) [3–5], Social Values for Ecosystem Services (SolVES) [6,7], Integrated Valuation of Ecosystem Services and Tradeoffs (InVEST) [8–10], Maxent Models [11,12], Artificial Intelligence Models (ARIES) [13], etc. There are significant differences in the areas to which different quantitative evaluation models apply and the functions they demonstrate. For example, the SolVES model evaluates the value of the region's cultural and social functions mainly from multiple perspectives [14,15]. The MAXENT model concentrates on assessing the research area's HQ from the standpoint of the species [16,17]. In contrast, the InVEST has a wide range of scales of application and good assessment results and offers solid assessment findings over a wide variety of application sizes [18,19]. This includes changes in water production [20], HQ [21–24], ecosystem services [25] etc.; it is applied in multi-scale studies, including land use [21,25–27], nature reserves [28], tourist attractions [29], watersheds [30,31], different regional scales [32,33] etc.. It is also highly suitable for analyzing changes in HQ across time and space [34] and for simulation prediction [32].

Investigation into the factors influencing changes in HQ is a key component in understanding the characteristics of changes in HQ and enhancing the status of HQ. Currently, analyses exploring the factors influencing changes in HQ fall into two categories, one based on geoprobes, geographically weighted regression (GWR), and other models exploring the contribution of driving mechanisms to the impacts on HQ [30]. HQ change is influenced by climate, water distribution, socio-economic conditions, and other factors, and the internal functions of influence are complicated, making it particularly important to systematically analyze the mechanisms driving HQ change. The driving force of HQ change are multifactorial and comprehensive, in which the driving factors include natural and anthropogenic influences such as land use, DEM, slope, rainfall, and temperature [35]. HQ-driven mechanisms are studied with geoprobes [30], GWR models, relevance analysis [21], and other methods. Among these, geoprobes are spatial analysis methods that measure the degree of spatial stratification inhomogeneity and are widely used to analyze climate change [36], vegetation change [37], and other areas.

Occupying a spot in northwestern China, Xinjiang is marked by a classic temperate continental climate. The region is rich in ecological elements and a variety of ecosystems. The overall ecological environment is constrained by an arid climate and a fragile ecological structure. Xinjiang is rich in mineral resources with high socio-economic value. Lately, the fast-paced progress in the Tianshan zone has increased the susceptibility of the ecological environment. ZHU et al. applied the InVEST to assess the spatiotemporal variations in ecosystem services within Xinjiang's nature reserves, discovering a positive link between economic progress and the effectiveness of soil and water conservation [38]. Hui et al. assisted in the management of ecosystems with the help of the InVEST system and showed that precipitation and temperature affect ecosystem benefits [39]. Kou et al. evaluated the

ecologically fragile Tuha region and proposed a new perspective for judging the equilibrium of economic interests and HQ, which reconciled the contradiction between the region's economic development and its fragile ecological environment [40]. Wei et al. evaluated the HQ of Wusu City and concluded that the adverse effects of anthropogenic factors on HQ was the greatest and could not be reversed [41]. As a crucial ecological bulwark in China, it is also important to analyze the changes in HQ of the northern slope of the Tianshan Mountains (NSTM). Lu et al. used the Tianshan Mountains in Xinjiang as the investigative domain and analyzed the changes in HQ in the Tianshan Mountains over the past two decades and its dominant factors by using the InVEST system and a geodetector [42]. Han et al. focused on the spatiotemporal variations in HQ in urban agglomerations on the NSTM and introduced partial least squares structural equation modeling to explore the interactions between natural and non-natural factors and their effects on HQ [43].

The NSTM is the only city cluster in the core zone of the Silk Road Economic Belt (SREB). With the implementation of China's "Western Development Strategy", the NSTM has become the most economically developed area in Xinjiang and an important hub of the SREB with a very important economic and locale. In parallel, the NSTM is also an important ecological barrier in Central Asia, and the quality of its habitats is critical for the protection of regional ecological balance and the spectrum of biodiversity. In recent years, the NSTM has experienced accelerated urban growth, industrialization, agricultural intensification, and other human activities, which have greatly affected the land use structure, causing various degrees of disturbance and damage to HQ. As the most direct and significant reflection of human activities on the natural environment, there is a close link between land use change and HQ change. Although previous studies have initially explored the HQ of NSTM, an in-depth understanding of its spatial and temporal differentiation characteristics and driving factors remains lacking. Previous researchers mainly studied the natural geographic region of the Tianshan Mountains and concluded that the influence of natural factors was stronger than human activities (the influence of the concentration of human activities around the Tianshan Mountains was not taken into account). In contrast, this paper focuses on economic–geographical divisions, examines the urban agglomeration on the northern slopes of the Tianshan Mountains, a key area for the development of China's Xinjiang, studies the harmony between economic development and the ecological environment in environmentally fragile zones, and explores the impact of human activities on the quality of habitats, arguing that the influence of topography and land use-type shifts is stronger. Within the scope of this article, rooted in the LULC of the NSTM from 2000 to 2020, we operated with the InVEST to assess the HQ in the study area, reveal its spatiotemporal variability characteristics, and explore the driving factors influencing HQ using geoprobes. The above research content is of great significance for understanding the mechanism of HQ change, assessing the health of ecosystems, and formulating scientific and reasonable ecological protection and restoration strategies. It also provides reference value for the central and local governments to formulate targeted policies.

2. Materials and Methods

2.1. Study Area

The NSTM is situated northwest of China (83°24′~91°34′ E, 42°55′~46°13′ N), encompassing an area of 1.24226×10^5 km^2, which represents 7.46% of Xinjiang. The study area is characterized by a continental arid climate, with terrain decreasing in altitude from south to northwest, forming a pincer-shaped encirclement, and an altitude ranging from 182 to 5251 m. The NSTM exhibits a considerable elevated span above sea level, which gives rise to distinctive topographical and geomorphological features. These include mountain ranges, intermountain plains, intermountain basins, and hills and valleys (Figure 1). The

municipalities on the NSTM comprise a total of eight urban areas and 25 districts and counties, indicating the regions in Xinjiang that are the most economically advanced and have the highest population density. Acting as a vital ecological barrier in the Xinjiang Uygur Autonomous Region, the HQ of the NSTM is crucial for maintaining the ecological balance of the region.

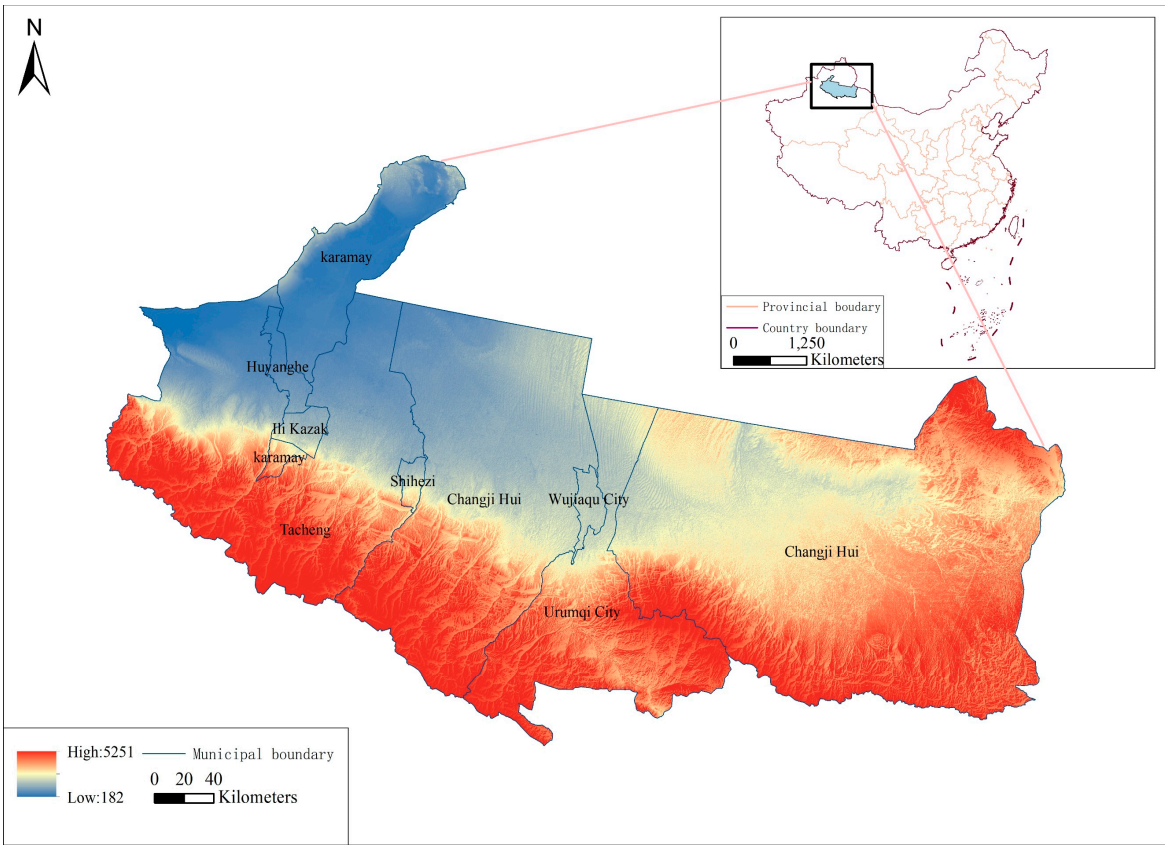

Figure 1. Study area: DEM of the north slope of Tianshan Mountain city cluster.

2.2. Database

The data utilized in this study included the 2000, 2005, 2010, 2015, and 2020 land use data of the NSTM. The Geospatial Data Cloud furnished the DEM data. Rainfall data, sourced from CRU TS, were provided by the NERC Centers for Atmospheric Science (UK) (NCA-S), consisting of monthly data covering the land surface at a 0.5° resolution from 1901 to 2023, available in NetCDF format. NDVI data were extracted from the Digital Earth Open Platform and selected from the 30 m NDVI dataset for China covering the years 2000 to 2020. The data format was GeoTIFF and ArcGIS grid format, in floating-point type, with a resolution of 30 m. Population density data were obtained from a global population data assessment initiated by the University of Southampton in 2013, with a resolution of 100 m. The data in this paper are categorized as shown in Table 1.

Table 1. Data source classification.

Data Type	Data Sources	Website Address	Spatial Resolution
Land use	Resource and Environmental Science Data Centre of the Chinese Academy of Sciences	http://www.resdc.cn/, accessed on 25 March 2024	30 m
DEM	Geospatial Data Cloud	http://www.gscloud.cn, accessed on 25 March 2024	30 m

Table 1. *Cont.*

Data Type	Data Sources	Website Address	Spatial Resolution
Rainfall	NERC Centers for Atmospheric Science (UK)	https://crudata.uea.ac.uk/cru/data/hrg/, accessed on 25 March 2024	0.5°
NDVI	Digital Earth Open Platform	https://open.geovisearth.com, accessed on 28 March 2024	30 m
Population	WorldPop	https://www.worldpop.org/, accessed on 28 March 2024	100 m

2.3. Methods

2.3.1. Dynamic Degree of Land Use

A depiction of the spatiotemporal progression of land use categories in the research area regarding individual land use changes and integrated land use changes is provided here [44]. The expression for the model is (Expression 1, Expression 2)

$$\text{Single dynamic degree}: K = \frac{U_b - U_a}{U_a} \times \frac{1}{T} \times 100\% \quad (1)$$

K represents the shift in orientation of a particular landform following the a-b interval; U_a and U_b, respectively, represent the area of the land category during periods a and b. T is the size of the study time. When K is greater than zero, it indicates that the landform area increased during the study period, and when K is less than zero, it indicates a decrease.

$$\text{Comprehensive dynamic degree}: L_c = \frac{\sum_{i=1}^{n} \Delta L_{uij}}{2\sum_{i=1}^{n} L_{ui}} \times \frac{1}{T} \times 100\% \quad (2)$$

L_c represents the combined dynamic attitude of land use in the study area; ΔL_{uij} denotes the difference in area between land class i and non-i land classes; and L_{ui} is the size of land class i in the initial period.

2.3.2. Land Transfer Matrix

The land use transfer matrix can characterize the structure of land use change on the NSTM [45]. The expression for the land use transfer matrix model is (Equation (3))

$$S_{ij} = \begin{bmatrix} S_{11} & S_{12} & \cdots & S_{1n} \\ S_{21} & S_{22} & \cdots & S_{2n} \\ \vdots & \vdots & \ddots & \vdots \\ S_{n1} & S_{n2} & \cdots & S_{nn} \end{bmatrix} \quad (3)$$

S_{ij} is the size of the area transferred from land type i to land type j in the study area; n denotes the quantity of land use categories within the research area. By analyzing the direction of land resource transfer and the amount of transfer, the pattern and amount of land use change in the study area can be clarified.

2.3.3. InVEST Habitat Quality Model

This paper is based on the HQ module of the InVEST to assess and analyze the NSTM. The approach involves identifying the sources of threats to HQ, determining the extent of habitat deterioration in the research area by establishing a functional relationship between HQ and threat factors, linking the extent of habitat degradation to the habitat suitability of each category within the region, and ultimately obtaining the final outcomes of the HQ

assessment for the research area [46]. The degree of habitat degradation is calculated as follows [47,48]:

$$D_{xj} = \sum_{r=1}^{R} \sum_{y=1}^{Y_r} \left(W_r / \sum_{r=1}^{R} W_r \right) r_y i_{rxy} \beta_x S_{jr} \quad (4)$$

D_{xj} represents the total threat level of the j-th type of threat source to the x grid; R signifies the count of threat sources; Y_r signifies the count of threat source r; W_r denotes the weight associated with threat source r; r_y is the value of raster y in threat source r; βx represents how accessible the threat source is to grid x. The value is from 0 to 1, with 1 indicating full exposure to the threat and 0 indicating full protection; S_{jr} indicates the susceptibility of type j to threat source r, ranging from 0 to 1; i_{rxy} is the degree of influence of the grid y on x. This includes the following two scenarios:

$$\text{Linear Decline} : i_{rxy} = 1 - \left(\frac{d_{xy}}{d_{rmax}} \right) \quad (5)$$

$$\text{Index Recession} : i_{rxy} = \exp\left(- \left(\frac{2.99}{d_{rmax}} \right) d_{xy} \right) \quad (6)$$

d_{xy} is the Euclidean distance between the grid y and x; d_{rmax} is the maximum extent of the action of the threat source r.

Finally, the degree of regional habitat degradation as a function of HQ was established and calculated as follows:

$$Q_{xj} = H_j \left(1 - \left(\frac{D_{xj}^z}{D_{xj}^z + k^z} \right) \right) \quad (7)$$

Q_{xj} signifies the HQ of grid x in type j; H_j denotes the habitat suitability for type j; z serves as the default parameter for normalizing the model (the Z value is usually taken as 2.5. The highest correlation between the model predictions and the degree of habitat degradation observed in the field was achieved when z was 2.5); and k, referred to as the half-saturation coefficient, defaults to 0.05, or it can be taken to be assigned to half the maximum value based on the degradation results of the first operation of the model. Included among these, Q_{xj} and H_j both take values in the range 0–1.

According to the data requirements of the InVEST, this paper, based on the reference to expert opinions and previous studies, selects arable land and construction land, which are more frequently interfered with by man and where human activities are most concentrated, as the main threat sources. At the same time, taking into account the regional characteristics of the northern slope of Tianshan Mountain, sandy land, Gobi, bare land, and other unused land, which account for a large proportion of the area of the region and result in substantial harm to the environment, are taken as the key objects to be analyzed. The layout of threat sources in the area is displayed in Figure 2. Finally, according to the manual for the use of the InVEST, the actual geographical conditions of the region and the relevant studies on HQ were integrated to determine the threat source attributes and the sensitivity values for each category [49–55]. See Appendix A for specific data (Tables A1 and A2).

2.3.4. Spatial Autocorrelation Analysis

This study was analyzed using the global Moran's index and local Moran's index. The Moran index reveals spatially clustered features of habitat quality by quantifying the similarity between spatial units. The global Moran's index is capable of determining whether habitat quality is spatially autocorrelated or not at an aggregate level. The local Moran index identifies areas where habitat quality is spatially clustered. On the overall

NSTM, the global Moran index is used in this paper to represent it [51]. Its calculation formula is as follows:

$$I = \frac{n}{\sum_{i=1}^{n}\sum_{j=1}^{n} w_{ij}} * \frac{\sum_{i=1}^{n}\sum_{j=1}^{n} w_{ij}(x_i - \overline{x})(x_j - \overline{x})}{\sum_{i}^{n}(x_i - \overline{x})^2} \quad (8)$$

n represents the overall count of spatial units. w_{ij} denotes the spatial adjacency weight between spatial units i and j. x_i and x_j represent the values of spatial i and j. $\overline{x}$ is the mean.

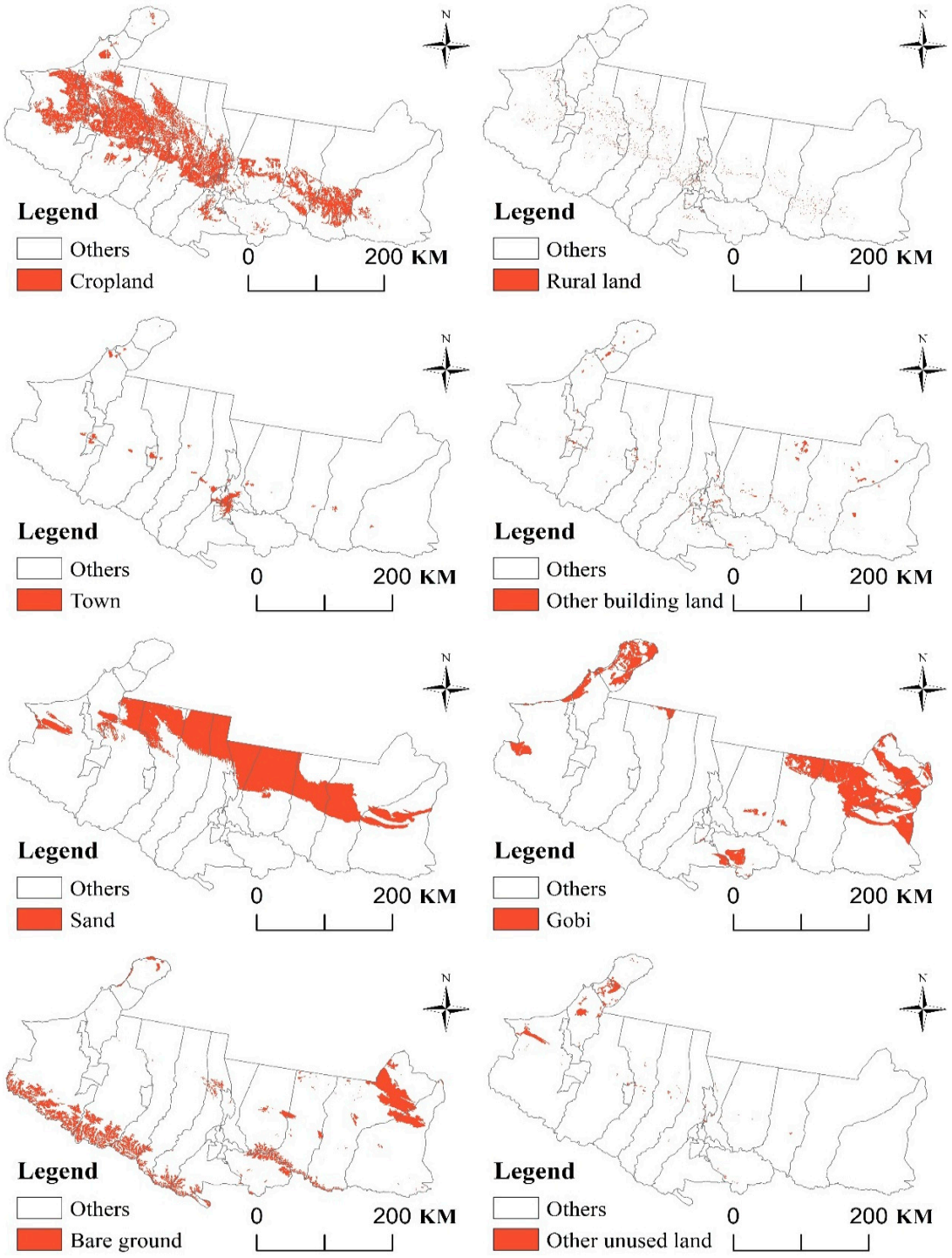

Figure 2. Spatial distribution of the different threat sources on the northern slopes of Tianshan Mountain, 2020.

Locally on the NSTM, this paper utilizes the local Moran's index [52], which is calculated using the following formula:

$$I_i = \frac{x_i - \overline{x}}{S_i^2} * \sum_{j=1, j\neq i}^{n} w_{ij}(x_j - \overline{x}) \tag{9}$$

$$S_i^2 = \frac{\sum_{j=1, j\neq i}^{n}(x_i - \overline{x})^2}{n-1} - x^2 \tag{10}$$

2.3.5. Geoprobe Model

This paper analyzes the possible driving factors in the study region by means of geo-detectors. The magnitude of the driving force of each driver is investigated, and the existence of a linear relationship that can cause a greater degree of change in HQ when the factors interact two by two is also explored [55]. The calculations are as follows:

$$q = 1 - \frac{\sum_{h=1}^{L} N_h \sigma_h^2}{N\sigma^2} \tag{11}$$

q indicates the magnitude of the driving force of the driver on the dependent variable, with values spanning from 0 to 1. The value's magnitude correlates with the effect's strength; L is the total number of partitions; N signifies the cell count throughout the study region; N_h is the number of cells in partition h; σ^2 is the variance of the dependent variable within the research region; and σ_h^2 is the variance of the h partition [56].

The research process of this paper is shown in Figure 3.

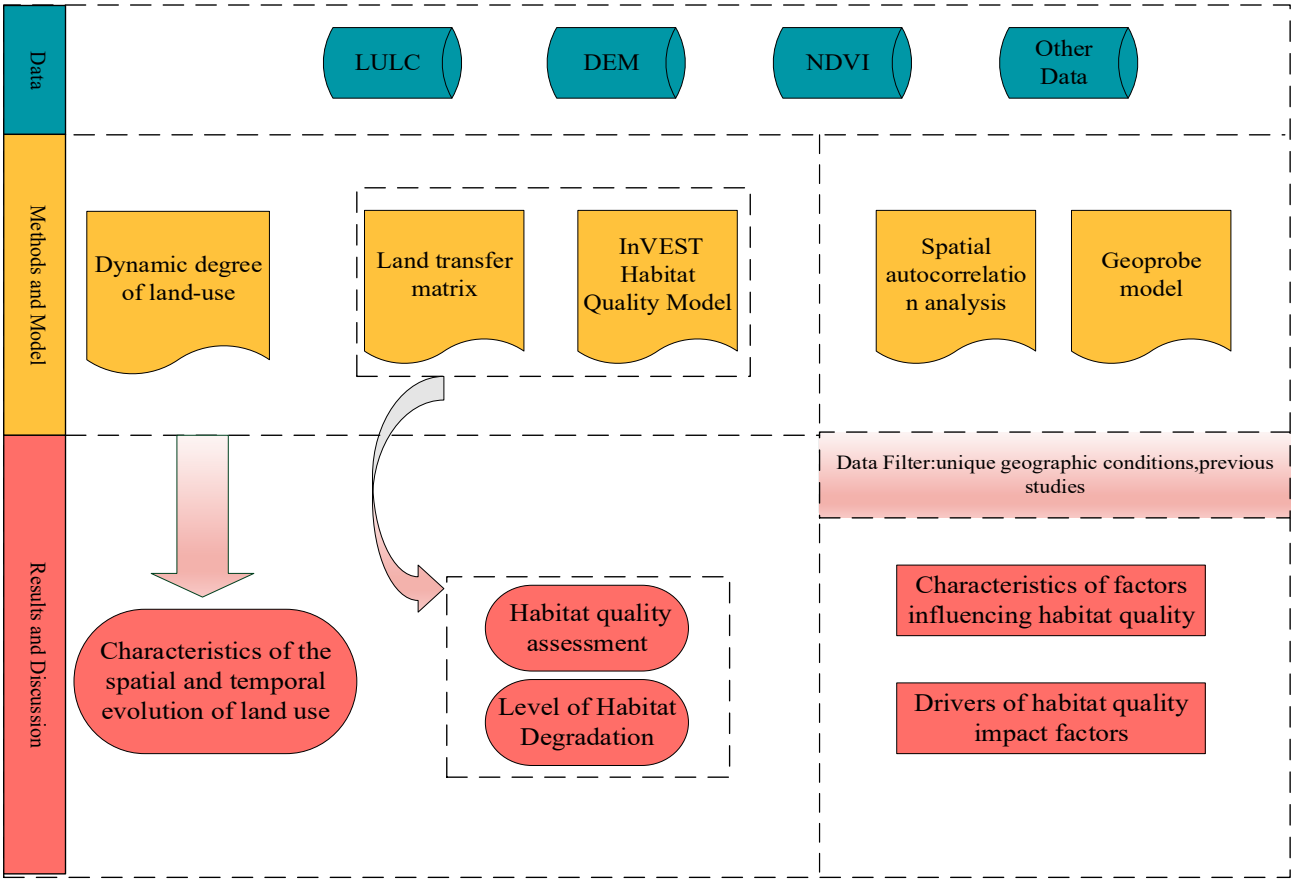

Figure 3. Overall study process.

3. Results

3.1. Characteristics of the Spatial and Temporal Evolution of Land Use

Spatially, there was a considerable shift in land use within the investigative domain between 2000 and 2020 (Figure 4), with a significant increase in the area occupied by arable land, built-up land, and unused land, and a sharp fall within the region belonging to forest land, grassland, and water. Among them, grassland and arable land showed the greatest change, with grassland decreasing from 42.92 percent to 38.89 percent, while the share of arable land area increased from 11.65 percent to 17.05 percent. The large-scale development of the urban agglomeration on the NSTM has led to a significant increase in the area of land used for urban construction by 1.50×10^3 km^2, and the appetite for arable land has broadened by 6.71×10^3 km^2 resulting from city development and a population surge (Table 2).

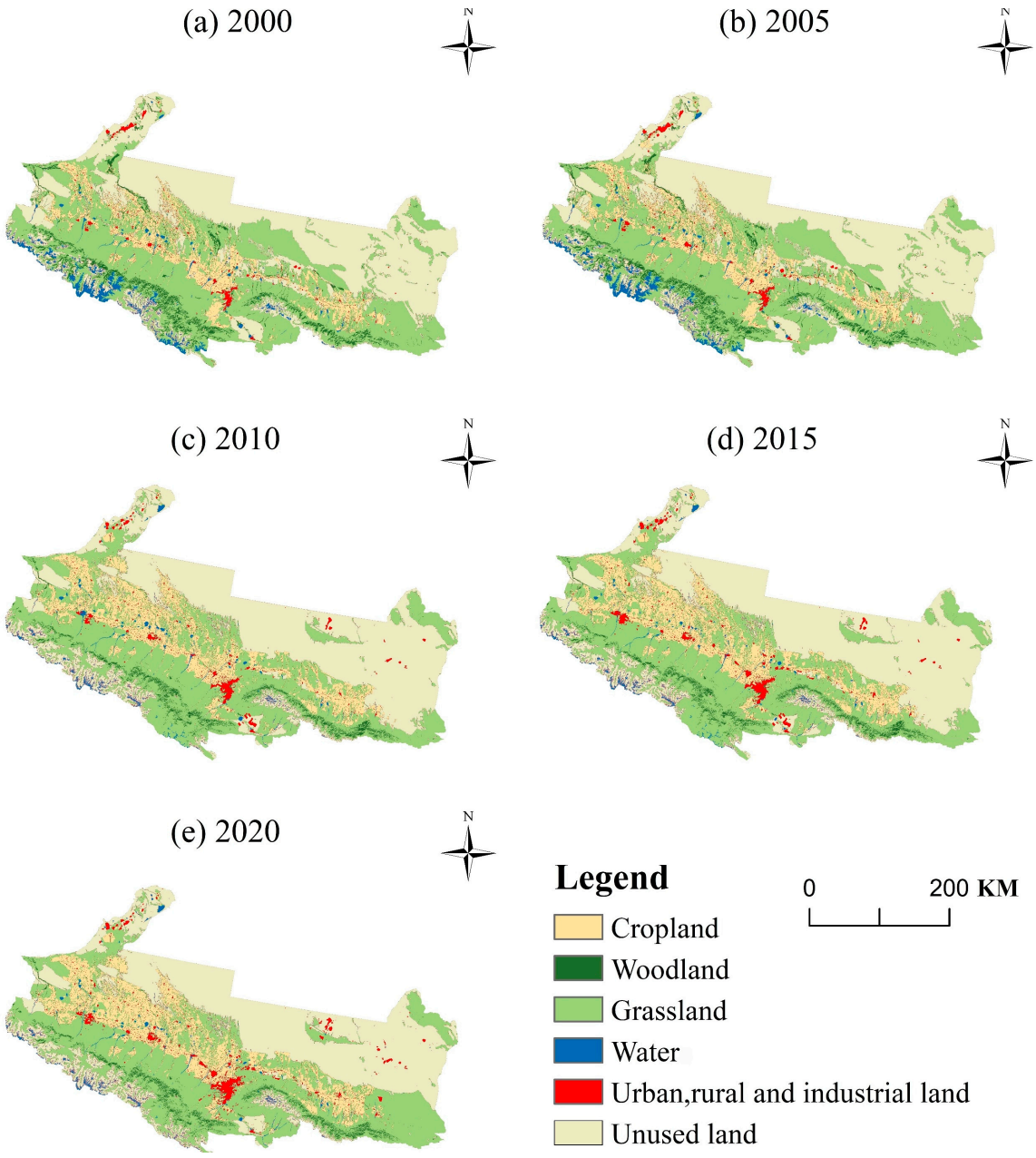

Figure 4. Spatial distribution of land use on NSTM, 2000–2020.

Table 2. Structure and proportion of land use on NSTM (10^3 km^2).

Land Type	2000		2005		2010		2015		2020		
	Area	**Percentage**	**Area**	**Percentage**	**Area**	**Percentage**	**Area**	**Percentage**	**Area**	**Percentage**	**Subtotal**
arable land	14.47	11.65%	15.44	12.43%	20.00	16.10%	20.35	16.38%	21.18	17.05%	6.71
woodland	4.94	3.97%	4.90	3.94%	2.64	2.13%	2.63	2.12%	2.51	2.02%	−2.42
grassland	53.32	42.92%	52.44	42.21%	47.19	37.98%	46.54	37.47%	48.31	38.89%	−5.00
body of water	3.28	2.64%	3.28	2.64%	1.78	1.43%	1.66	1.33%	1.69	1.36%	−1.59
building site	1.49	1.20%	1.62	1.30%	2.10	1.69%	2.57	2.07%	2.99	2.41%	1.50
unused land	46.7	37.62%	46.55	37.47%	50.53	40.67%	50.48	40.64%	47.55	38.27%	0.81

In the sphere of land use dynamics (Table 3), the combined dynamics on the NSTM are small, and the overall change is relatively smooth. Among them, the highest comprehensive dynamic was in 2005–2010, reaching 1.45%, during which the land use categories in the research region changed drastically. From the perspective of single-dynamic motivation, it can be seen that during the period of 2005–2010, the motivation attitude of forest land and water areas was −9.22% and −9.14%, while for cultivated land and construction land, it was 5.90% and 5.88%, respectively. In addition, the single-motivation attitude of cultivated land and construction land was consistently positive, while that of forest land was negative, further indicating that the influence of anthropogenic factors has been increasing in the NSTM. This trend also indirectly reflects that the urban agglomeration on the NSTM is expanding.

Table 3. Single/comprehensive land use dynamics, 2000–2020.

	Land use type	2000–2005	2005–2010	2010–2015	2015–2020
Single-dynamic motivation	arable land	1.35%	5.90%	0.35%	0.82%
	woodland	−0.16%	−9.22%	−0.06%	−0.89%
	grassland	−0.33%	−2.00%	−0.27%	0.76%
	body of water	0.00%	−9.14%	−1.40%	0.38%
	building site	1.75%	5.88%	4.48%	3.30%
	unused land	−0.08%	1.71%	−0.02%	−1.16%
comprehensive dynamic		0.18%	1.45%	0.13%	0.49%

As shown in Figure 5, the overall degree of land use transfer in the region on the NSTM is weak, and land use transfer occurs mainly between grassland, cropland, and unused land, while the transfer of watersheds and forested land is relatively small. The data (see Table A3 in Appendix A for specific data) show that land use shifted drastically from 2005 to 2010. Among these changes, grassland was transferred to unused land by 11.10 × 10^3 km^2 and to arable land by 4.03 × 10^3 km^2, indicating that grassland was reclaimed to meet the demand for arable land due to population changes during this period, and that there was a significant desertification of grassland in the study area's ecological environment. Additionally, unused land was transferred to grassland by 7.00 × 10^3 km^2, indicating that during the process of urbanization and development on the NSTM, certain ecological restoration measures were taken, which contributed to maintaining the region's ecological balance.

3.2. Habitat Quality Assessment of the Northern Slopes of the Tianshan Mountains

The study's conclusions demonstrated that the overall HQ on the NSTM was low and declining year by year (Table 4), with significant spatial heterogeneity (Figure 6), characterized by "high in the south and low in the north". Among them, the distribution of inferior habitats is primarily in the north of the northwestern–southeastern belt and the southwestern border, mostly consisting of cultivated land, construction land, and unused land. High-grade habitat is concentrated in the south of the northwestern–southeastern

belt of the study area, mostly covering forest and grassland in the northern foothills of the Tianshan Mountains. Only the areas of the low-grade and lower-grade types increased from 2000 to 2020, while the areas of the remaining three types decreased to varying degrees, and the overall HQ was lower than that of the low grade. The average quality decreased by 3.2 percent, indicating an overall trend of ecological degradation on the NSTM.

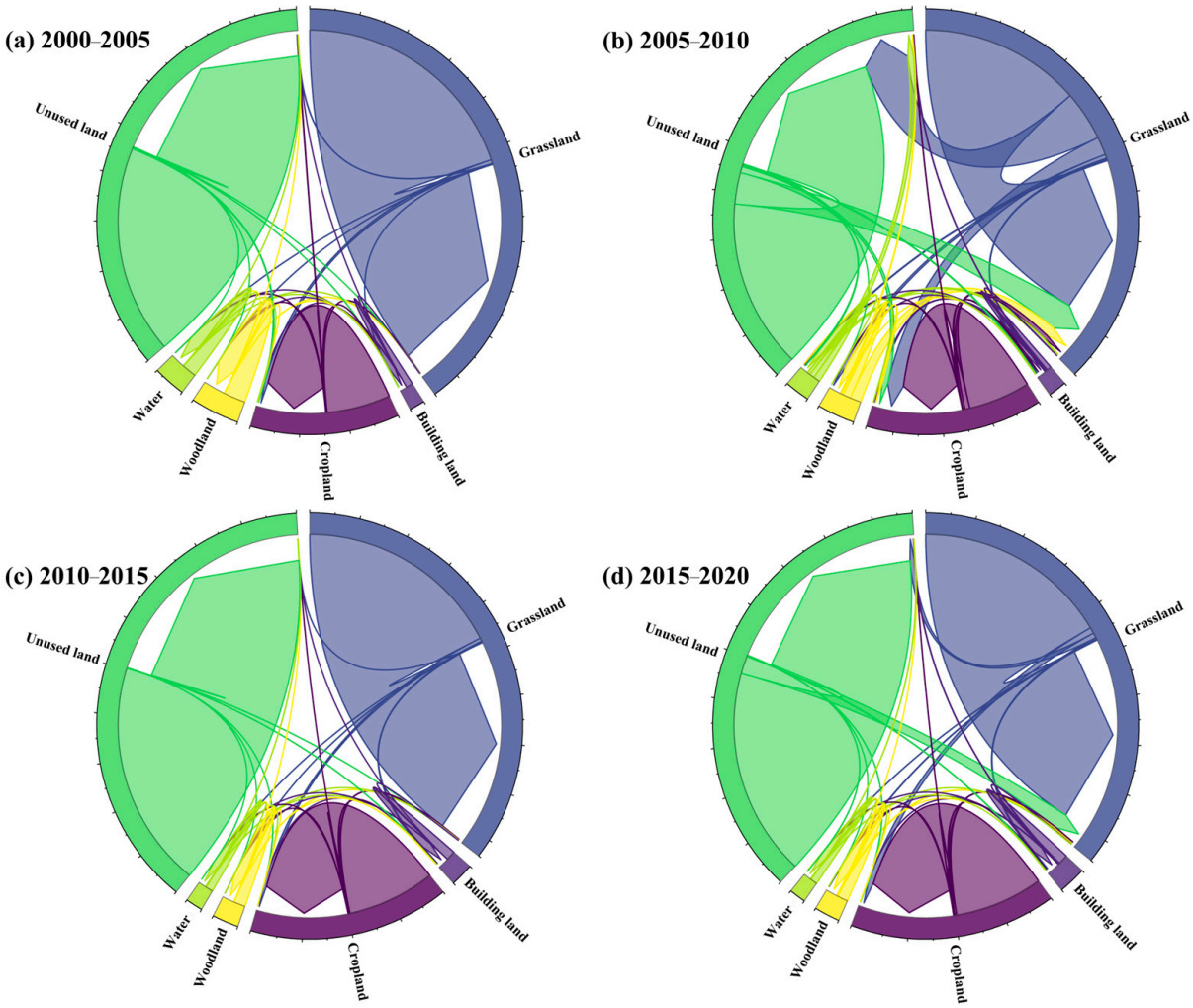

Figure 5. Land use transfer map, 2000–2020.

Table 4. Changes in HQ on the northern slopes of the Tianshan Mountains (10^3 km^2).

Habitat Quality	2000		2005		2010		2015		2020		Subtotal
	Area	Percentage	Area	Percentage	Area	Percentage	Area	Percentage	Area	Percentage	
Lowest level	69.64	56.06%	69.93	56.30%	74.23	59.75%	74.95	60.34%	74.75	60.17%	5.11
Lower level	15.17	12.21%	15.93	12.82%	17.71	14.25%	17.29	13.92%	16.26	13.09%	1.09
Medium level	6.81	5.48%	6.72	5.41%	6.58	5.30%	6.43	5.18%	6.08	4.89%	−0.73
Higher level	15.96	12.85%	15.15	12.20%	11.10	8.94%	10.97	8.83%	13.12	10.56%	−2.84
Top level	16.65	13.40%	16.49	13.27%	14.61	11.76%	14.57	11.73%	14.02	11.29%	−2.62
On average	0.33		0.32		0.29		0.29		0.29		

Analyzing the changes in HQ, one can observe (Figure 7) that the overall HQ of the NSTM showed a declining trend. Of these alterations, the territory with improved HQ stretched over 4.73 × 10^3 km^2, largely found in the eastern district of Changji Hui Autonomous Prefecture in the eastern section of the study area, the western part of the Tacheng area, and the southern part of the Tianshan Mountains. The fact that such results

have been achieved is largely due to the efforts of the local government sector. The quality of the environment has been improved through the implementation of a series of policies and governance measures, such as the Wetland Conservation and Restoration Program.

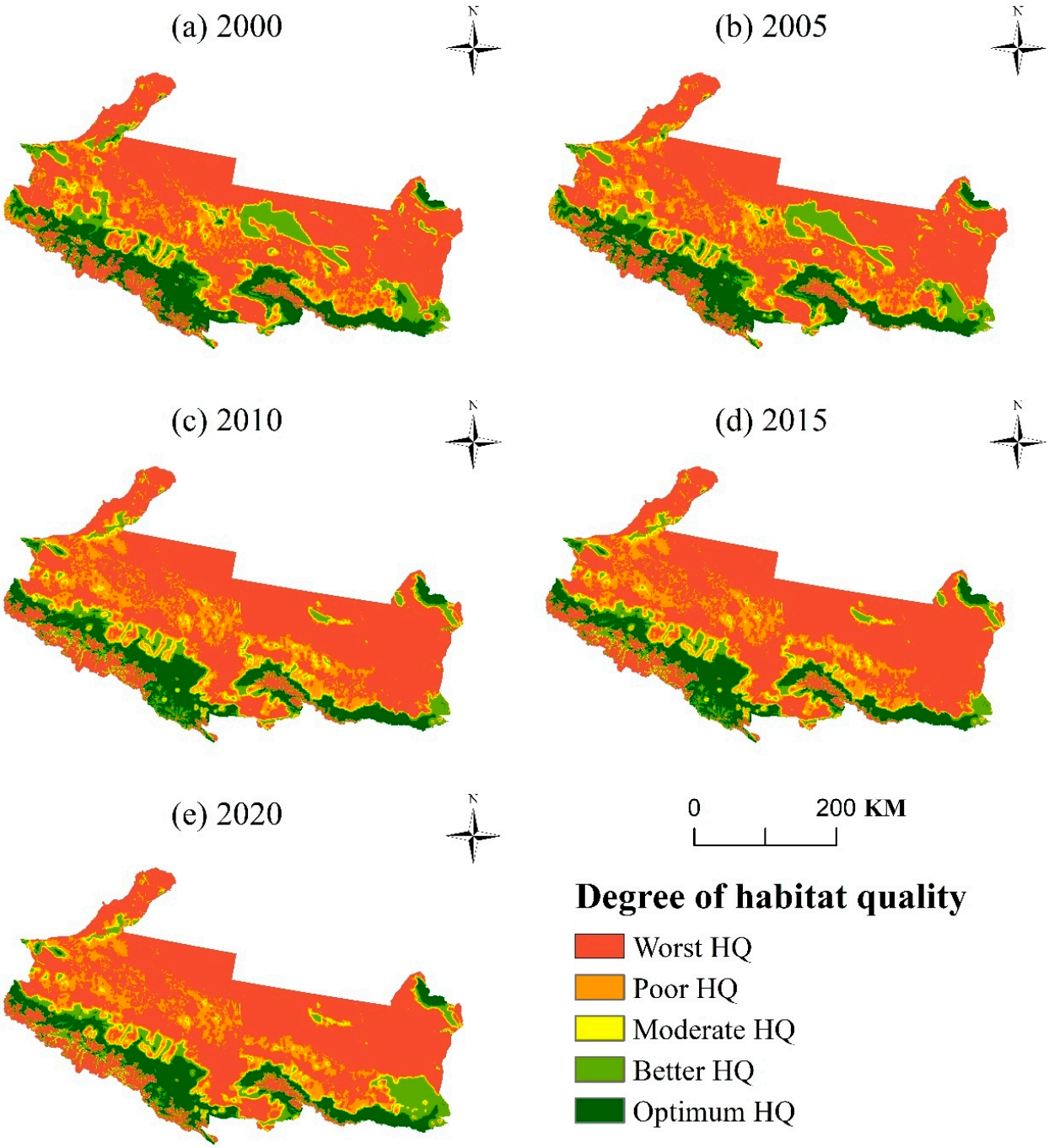

Figure 6. Spatial and temporal distribution of HQ on NSTM, 2000–2020.

The area where HQ decreased was 67.78 × 10^3 km^2, mainly focused in the urban clusters of Urumqi, Shihezi, Karamay, and Ili Kazakh Autonomous Prefecture. The expanse with the least change in HQ, covering 9.92 × 10^3 km^2, was mainly located in the northern and southern zones of the research region. This stems from the NSTM being adjacent to the Gurbantunggut Desert in the north, with harsher geographic conditions, and to the Tianshan Mountain Range in the south, with more favorable natural conditions, generally higher elevations, and fewer human interventions, which allowed the HQ to remain stable.

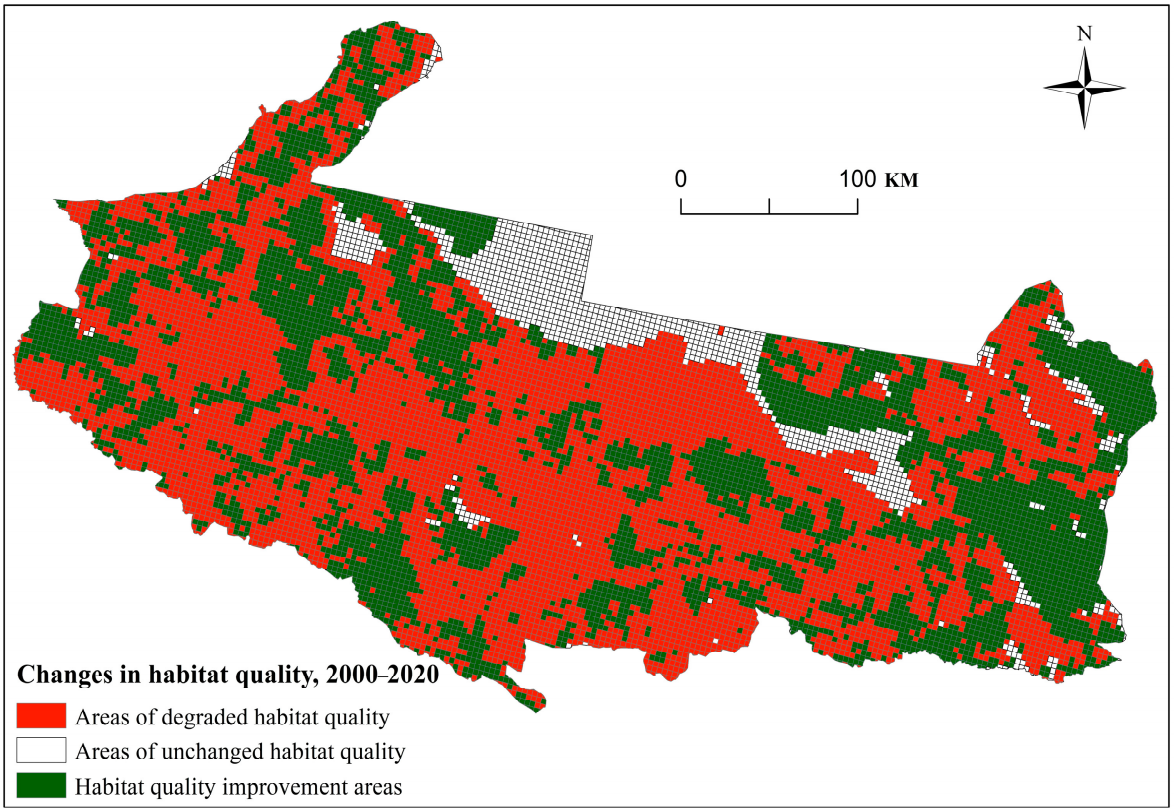

Figure 7. Changes in HQ on NSTM.

3.3. Level of Habitat Degradation on the Northern Slope of Tianshan Mountains

The extent of habitat degradation correlates with the level of impact that threat sources have on the region, and its high or low value characterizes the potential status of ecological damage in the region. It is an attribute, not a state quantity. Specifically, it describes the ecological sensitivity of the area and does not indicate that the ecosystem is experiencing structural damage, functional decline, etc. Habitat degradation on the NSTM is relatively poor (less than 0.027), showing a clear radial structure, with low degradation at the margins and high degradation at the nucleus (Figure 8). Among them, weak deterioration is dispersed over the research area and takes up the most space, where the environment is relatively stable, consisting mainly of grassland, woodland, and unused land. On the other hand, habitat degradation is significantly higher in the central area, mostly made up of construction land and arable land and where human activity is frequent and where strong ecological interference and a more fragile environment exist.

As shown in Table 5, only the more strongly degraded areas increased in the study area, while the remaining three categories all showed varying degrees of shrinkage, and the ecological environment on the NSTM became increasingly fragile by 2020. During the period from 2000 to 2020, the level of habitat deterioration on the NSTM exhibited a "increasing-decreasing-increasing" pattern, with the lowest average habitat degradation occurring in 2010 and the greatest in 2020. Among them, the period from 2015 to 2020 is the most significant, with the cities of Karamay, Shihezi, and Urumqi serving as axes for outward expansion, increasing the level of habitat degradation, while the radial structure gradually appears in the southeast. Combined with the LULC (Table A4), the development of the three central urban agglomerations further drove the economy of surrounding areas, including the gradual development of remote villages and the regional energy sector, thus contributing to habitat degradation.

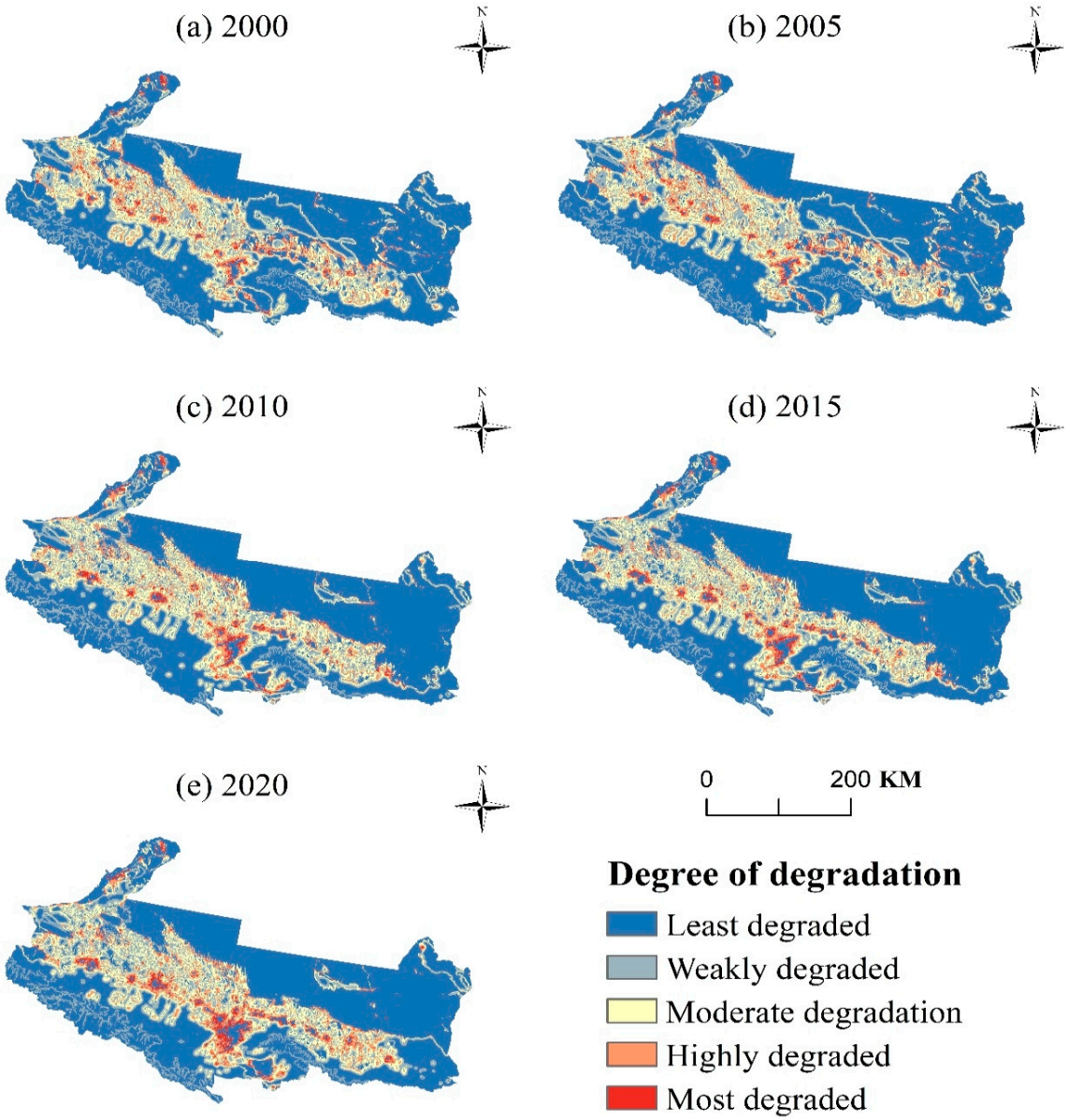

Figure 8. Spatial and temporal distribution of habitat degradation on NSTM, 2000–2020.

Table 5. Changes in habitat degradation on the northern slopes of Tianshan Mountains (10^3 km^2).

Degree of Habitat Degradation	2000		2005		2010		2015		2020		Subtotal
	Area	Percentage	Area	Percentage	Area	Percentage	Area	Percentage	Area	Percentage	
Least degraded	72.51	58.37%	72.14	58.07%	72.43	58.31%	73.84	59.44%	72.49	58.35%	−0.03
Weakly degraded	21.59	17.38%	21.33	17.17%	20.23	16.29%	19.84	15.97%	20.21	16.27%	−1.34
Moderate degradation	19.58	15.76%	19.71	15.87%	20.65	16.63%	20.20	16.26%	19.43	15.64%	−0.15
Highly degraded	8.50	6.85%	9.06	7.29%	8.44	6.79%	8.14	6.56%	9.22	7.42%	0.72
Most degraded	2.04	1.64%	1.99	1.60%	2.47	1.99%	2.19	1.77%	2.88	2.32%	0.84
On average	0.02		0.03		0.02		0.02		0.03		

4. Discussion

4.1. Characteristics of Factors Influencing Habitat Quality

To investigate the causes of spatial patterns of HQ on the NSTM, this paper considers the unique geographic conditions of the region and the existing findings of previous studies [57–60]. Five categories of influences, including natural drivers (elevation, slope, rainfall) and anthropogenic drivers (population density, normalized difference vegetation

index (NDVI)), were screened and categorized for discussion. In addition to this, additional LULC impact factors were added for categorical discussion.

The six factors of HQ in the study area exhibit a distinct spatial distribution pattern (Figure 9). Among them, the southern area has steeper slopes and higher elevations, whereas the northern area has more gradual slopes and lower elevations; the cities of Urumqi, Shihezi, and Karamay are the primary locations for the population. The northwestern and eastern regions receive less rainfall and are mostly unused land, while the central and southwestern regions receive more rainfall and are predominantly forested, grassland, and cropland. This also results in higher vegetation cover along the northwestern and southeastern locations within the research locale.

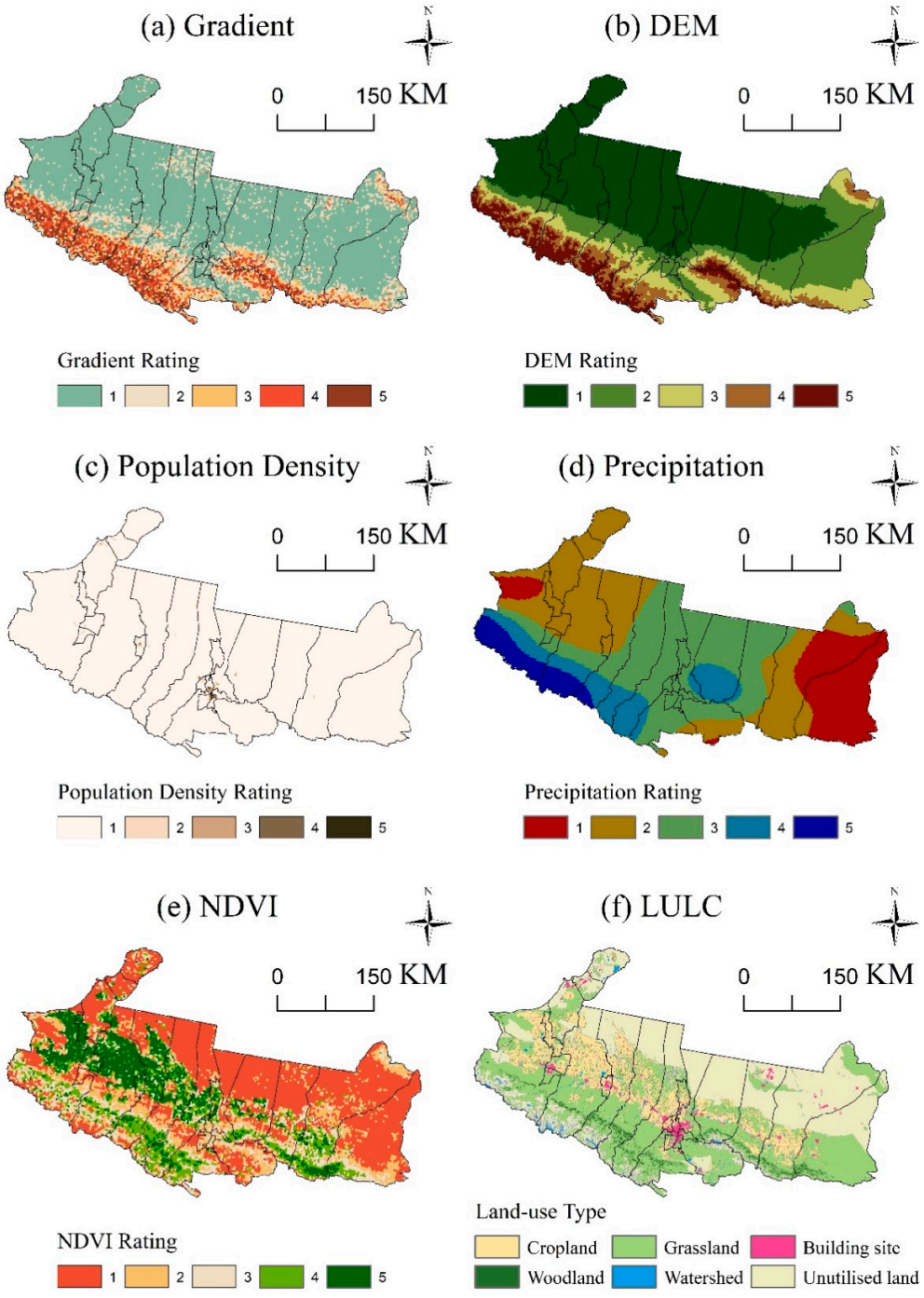

Figure 9. Spatial distribution patterns of factors affecting HQ (2020).

Further study of the first five categories of factors reveals a clear pattern of change in HQ corresponding to each gradient as the gradient increases. The results showed that the fifth gradient accounted for a smaller area in the study area. Except for rainfall, the other four types of factors were dominated by the first gradient, with the population density of the first gradient occupying almost the entire study area, while rainfall was mainly concentrated in the second and third gradients.

The findings obtained from Pearson's correlation analysis pointed out that among the five types of factors, only the HQ associated with population density was negatively correlated with the gradient, while the HQ of the other four factors was positively correlated with the gradient (Figure 10). This indicates that HQ increased with the gradient. Among these, slope gradient had the highest positive correlation (0.766), suggesting that ecological conditions were poorer in low-gradient areas, whereas HQ was better in moderate-gradient areas, which are more suitable for organism survival. Population density showed the highest negative correlation (−0.742), revealing that HQ was better in areas with lower population density in the study area, highlighting the significant influence of anthropogenic factors on HQ. Additionally, vegetation cover had the smallest correlation (0.307). The pattern of HQ changes in DEM and the NDVI showed a significant correlation (0.891). Most areas with better HQ in NDVI gradients overlapped with areas of better HQ in DEM gradients. The combined curves showed that HQ was better in areas with higher elevations, where there are fewer disturbances and conditions are suitable for large-scale vegetation growth, resulting in higher vegetation cover. Also, when analyzed in conjunction with Figure 6 and the DEM, habitat quality is good at higher elevations and poor at lower elevations. This can reflect that the habitat quality in the study area is mainly determined by the spatial distribution of elevation.

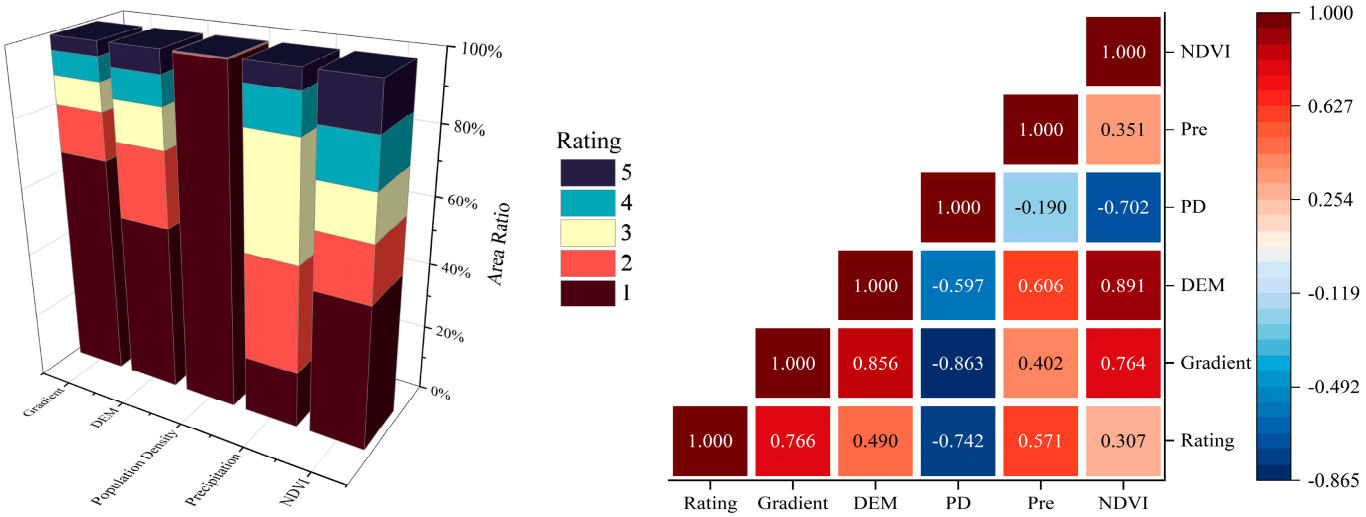

Figure 10. Area share and Pearson's correlation analysis.

4.2. Study of the Drivers of Habitat Quality Impact Factors

The analysis conducted by the geoprobe showed that HQ on the NSTM was mainly influenced by elevation (0.4973) and land use type (0.3654), followed by slope, the NDVI, rainfall, and population density (Figure 11).

Among them, DEM characterizes the regional altitude. Since the study area is situated in the northwest inland, the altitude span is extremely large, and the natural distribution of organisms is closely related to altitude. The high-altitude areas are primarily the Tianshan mountain range, while the low-altitude areas are mainly the Gurbantunggut Desert. Both feature harsh natural conditions and extreme ecological environments, resulting in lower

biodiversity. In contrast, areas with moderate altitude are more suitable for the survival of organisms. Therefore, the spatial distribution of DEM is crucial for the quality of habitats in the area, playing a dominant role in determining HQ.

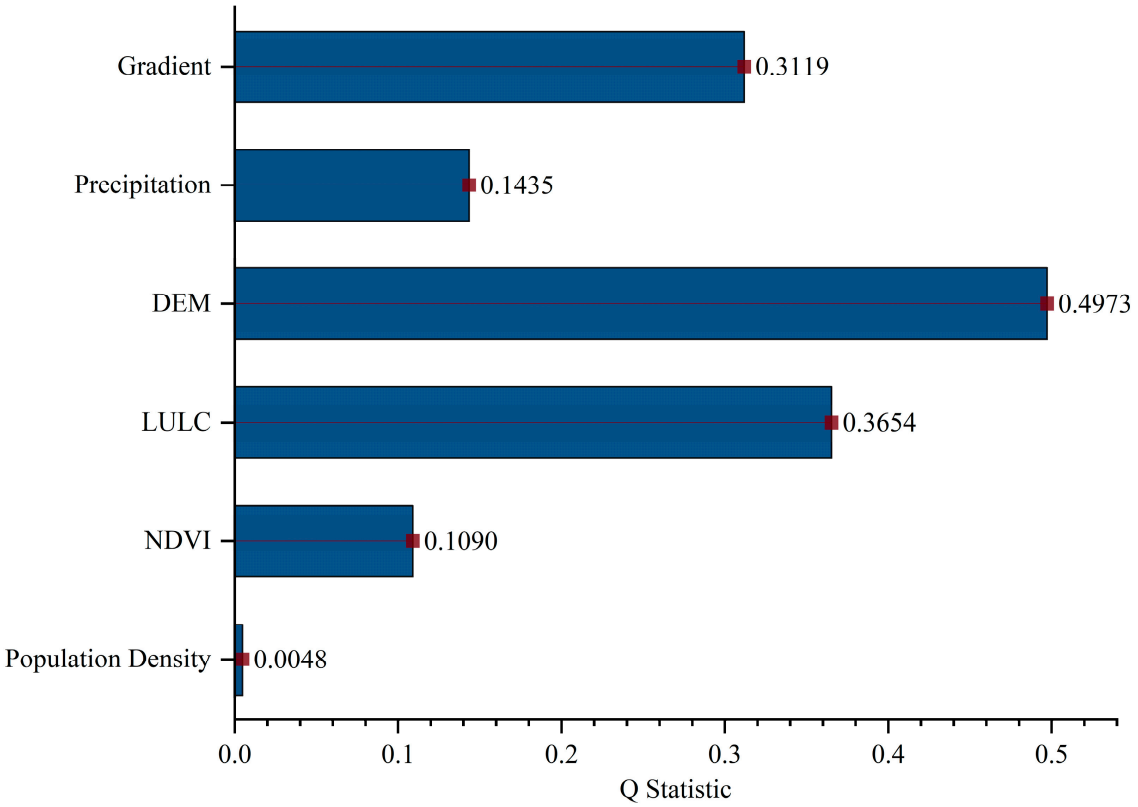

Figure 11. Results of single-factor detection by geodetector.

Land use types are affected by a blend of socio-economic and natural factors. Among them, the HQ of arable land and construction land is inadequate. With the development and expansion of western cities, the growth of urban agglomerations centered around Urumqi, Shihezi, and Karamay has further reduced the HQ of the three central cities and their surroundings, gradually threatening forested and grassed areas. At the same time, extreme natural environments such as deserts and the Gobi, which are widely distributed throughout vast regions of unused land, have also seriously affected the HQ pattern of the NSTM. Despite low levels of human intervention, the HQ in these areas in these regions has remained poor over time, and the ecosystem services functions are weak.

To further scrutinize the effects resulting from the interaction of multiple factors on the HQ within the research region, the conclusions drawn were that for the spatial distribution pattern of HQ on the NSTM, the interaction of any two factors exhibited non-linear enhancement without a relationship of mutual independence or weakening. This means that the driving force behind any two factors interacting was stronger than the force behind any one element acting alone, suggesting that the spatial distribution pattern of HQ on the NSTM is driven by multiple factors. This implies that the spatial pattern of HQ on the NSTM results from the collective effect of several factors. The interplay between DEM and land use had the most substantial impact on the HQ of the NSTM (0.6414), followed by slope and land use (0.5587) and DEM and rainfall (0.5558) (Figure 12). Meanwhile, the interaction results between DEM and the remaining factors were generally high (all greater than 0.49), suggesting that the regional spatial arrangement of elevation on the NSTM plays a very important role in the ecosystems of the entire NSTM. That is, it determines the spatial pattern of HQ on the NSTM to a certain extent.

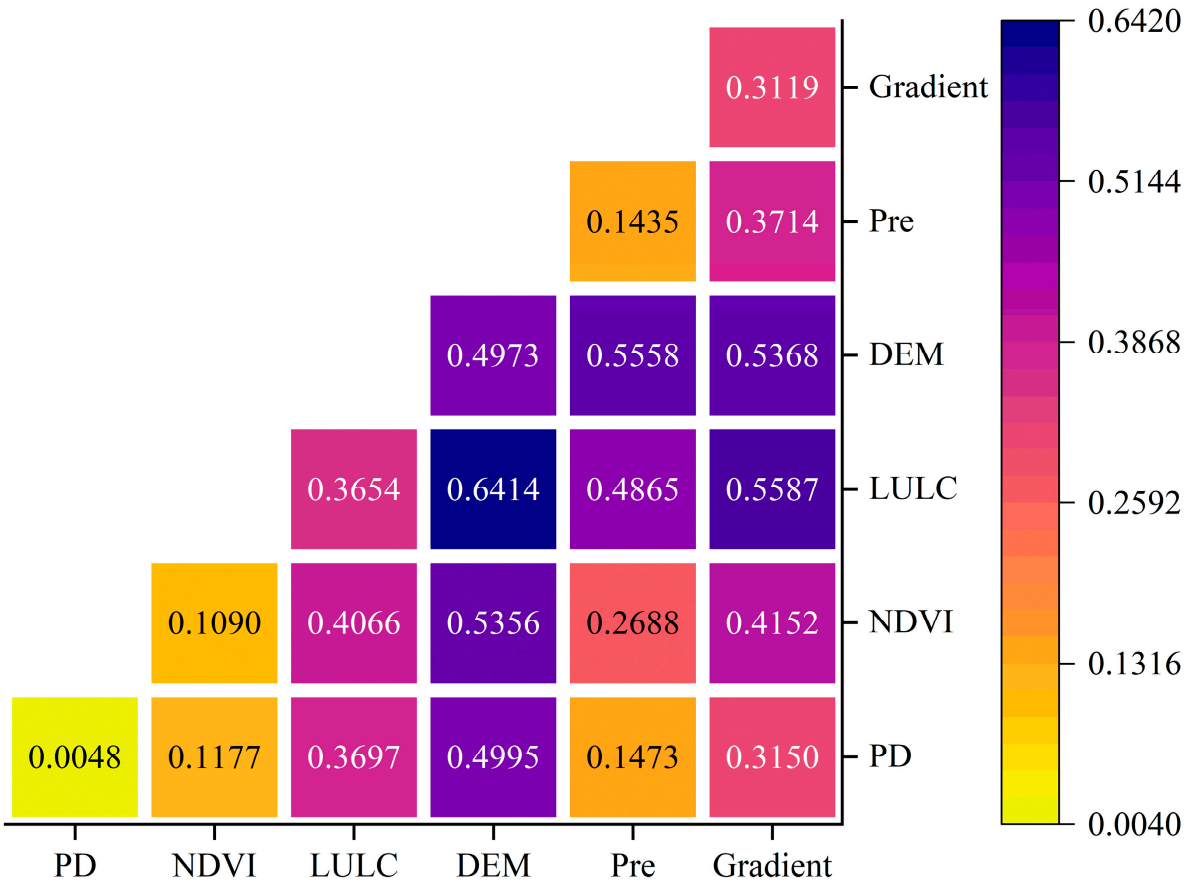

Figure 12. Geo-detector two-factor detection results.

4.3. Limitations and Outlook

The study in this paper only considered spatial heterogeneity on a single scale and did not consider the problem from a multi-scale perspective. Secondly, the parameter settings in a geodetector are subjective and must be referred to previous studies, with no indicators of uniformity. In addition to this, the findings of this paper are only regionally specific and cannot be applied to, for example, the Yangtze River Economic Belt [61], highly urbanized Shenzhen [62], the tropical rainforests of Cambodia [63], and so on. However, the application of the research methodology in terms of other models and other studied areas is equally valuable. The InVEST model and species distribution models (SDMs) were combined to predict the habitat suitability of 29 bird species in Italy with high accuracy [64]. In different research areas, such as remote sensing, modeling the ecological quality of the Bengal tiger using high-accuracy remote sensing imagery and random forest algorithms and simulations using the InVEST model is important for animal conservation [65].

5. Conclusions

This paper assesses the spatiotemporal progression of land use types on the NSTM, leveraging LULC data from 2000, 2005, 2010, 2015, and 2020 while assessing the HQ by using the InVEST and filtering six influencing factors, namely elevation, slope, rainfall, land use, population density, and the NVDI, by using a geoprobe. The key drivers of the spatiotemporal variation pattern in HQ within the study area were investigated. The study yielded the following primary conclusions:

(1) The land use types on the NSTM from 2000 to 2020 were dominated by grassland, unused land, and arable land, covering more than 90 percent of the total region. During the study period, the domain of farmable land and construction zones persisted in its

expansion, and the expansion trend was obvious, with the percentage of arable land rising from 11.65% to 17.05% and the proportion of construction land expanding from 1.20% to 2.41%. Simultaneously, the transformation in the comprehensive land use dynamics within the study area was quite limited, and the rate of land use conversion was relatively smooth. From the perspective of the single motive, the evident trajectory of expanding farmable and built-up land is accompanied by a steady decline in forest area. Land use change is mostly manifested in the shift in grassland and forest land to arable land, construction land, and unused land.

(2) The HQ of the NSTM from 2000 to 2020 was generally poor, dominated by a low grade with a clear distribution pattern of north–south differences. The lower grades were predominantly concentrated in the northern region of the north–west–south–east belt, mostly in arable land, construction land, and unused land. On the other hand, the higher grades are mainly clustered south of the north–west–south–east belt, consisting mostly of woodland and grassland. On the time scale, there is a "decrease followed by an increase", and the quality of habitats shows a trend of degradation.

(3) The spatial pattern of habitat degradation on the NSTM from 2000 to 2020 shows a significant radial structure, with low degradation at the edges and high degradation in the center. Habitat deterioration within the research region shows a progression in the direction of "increasing-decreasing-increasing" over time. Overall, the highest average habitat degradation was in 2020, and the lowest was in 2010, indicating that the ecological environment in 2010 was more stable, while the ecological environment in 2020 was more susceptible to disturbance by external factors.

(4) Regarding the influencing factors of HQ, according to the results of multi-factor interaction detection, one can observe that the spatial arrangement of habitat quality in the NSTM is not shaped by one factor alone but is the result of multiple factors driving the results together. Among these, the highest results of the interaction detection between the DEM and the land use type show the strongest driving effect on the HQ of the study area, and the results of the interaction detection between the DEM and its residual factors are generally high, indicating that the HQ in the study area was mainly determined by the spatial distribution of elevation. Therefore, the research area should emphasize the actual spatial layout of altitude in the locale and consider the planning of land use sorts so as to adopt relevant ecological environmental protection measures and formulate reasonable habitat protection policies.

Author Contributions: Conceptualization, R.W. and H.Z.; methodology, R.W. and H.Z.; data curation, M.C.; writing—original draft preparation, R.W., H.Z. and M.C.; writing—review and editing, H.Y., H.C. and Z.Y.; validation, R.W. and W.W.; resources, H.Y., Z.Y. and W.W. All authors have read and agreed to the published version of the manuscript.

Funding: This research was funded by the Third Comprehensive Scientific Investigation Project in Xinjiang (2022xjkk1006); the Xinjiang Uygur Autonomous Region Key Research and Development Program (2022B01012-1, 2022B01012-2); the Special Fund Project for Geological Exploration Construction and Development in Shanxi Province—Open Fund of Shanxi Geoscience Think Tank (2023-008); and the Science and Technology Innovation Project of Jiangsu Provincial Department of Natural Resources (2022008).

Data Availability Statement: The data presented in this study are available upon request from the corresponding author due to privacy.

Conflicts of Interest: The authors declare no conflicts of interest.

Appendix A

Table A1. Table of threat source attributes for the northern slopes of the Tianshan Mountains.

Source of Threat	Maximum Impact Distance/km	Weights	Recession Function
Cropland	6	0.6	Linear
Urban land	8	0.8	Exponential
Rural settlements	6	0.6	Exponential
Other construction land	7	0.7	Exponential
Sandy land	6	0.6	Exponential
Gobi	5	0.6	Exponential
Bare ground	5	0.5	Exponential
Other unused land	4	0.4	Linear

Table A2. Sensitivity of different land classes to different threat sources on the northern slopes of Tianshan Mountains.

Land Use Type	Habitat Suitability	Arable Land	Town	Rural Settlements	Other Building Land	Sand Field	Gobi (Desert)	Bare Ground	Other Unused Land
Paddy field	0.4	0	0.5	0.7	0.6	0.2	0.2	0.1	0
Dryland	0.3	0	0.5	0.6	0.5	0.3	0.3	0.2	0.1
Wooded land	1	0.7	1	0.8	0.6	0.5	0.5	0.4	0.4
Shrubland	1	0.6	0.8	0.7	0.6	0.6	0.6	0.5	0.3
Open woodland	0.9	0.7	0.9	0.8	0.7	0.7	0.7	0.6	0.4
Other woodland	0.8	0.6	0.8	0.7	0.6	0.6	0.6	0.5	0.3
High-cover grassland	0.9	0.5	0.7	0.6	0.5	0.4	0.4	0.3	0.3
Medium-cover grassland	0.8	0.5	0.6	0.5	0.4	0.5	0.5	0.4	0.2
Low-cover grassland	0.7	0.4	0.5	0.4	0.3	0.6	0.6	0.5	0.1
River and canal	1	0.6	0.9	0.7	0.5	0.5	0.5	0.4	0.4
Lakes	1	0.6	0.9	0.7	0.5	0.5	0.5	0.4	0.4
Reservoirs and ponds	0.9	0.7	0.8	0.6	0.4	0.6	0.6	0.5	0.3
Glaciers	0.1	0.2	0.2	0.1	0.1	0.1	0.1	0.1	0.1
Beaches	0.9	0.7	0.8	0.6	0.4	0.6	0.6	0.5	0.3
Urban land	0	0	0	0	0	0	0	0	0
Rural land	0	0	0	0	0	0	0	0	0
Other building land	0	0	0	0	0	0	0	0	0
Sand	0.1	0.1	0	0	0	0	0	0.1	0.1
Gobi	0.1	0.1	0	0	0	0	0	0.1	0.1
Salt and alkaline land	0.1	0.2	0.2	0.1	0.1	0.2	0.2	0.1	0.1
Marshland	0.4	0.6	0.6	0.5	0.4	0.4	0.4	0.3	0.3
Bare land	0.1	0.1	0	0	0	0.1	0.1	0	0.1
Bare rocky ground	0.1	0.1	0	0	0	0.1	0.1	0	0.1
Other unused land	0.2	0.3	0.2	0.1	0.1	0.1	0.1	0.1	0

Table A3. Land use transfer matrix 2000–2020 (km^2).

Year	Land Use Type	Grassland	Building Site	Arable Land	Woodland	Body of Water	Unused Land
2000–2005	Grassland	52,229.05	43.89	843.95	45.35	44.44	111.45
	Building land	2.45	1481.15	2.70	0.48	0.14	3.14
	Cropland	113.97	34.10	14,196.88	0.75	2.85	119.42
	Forest land	25.92	2.89	61.15	4839.57	4.04	2.51
	Water	33.40	1.07	3.57	1.68	3206.49	31.30
	Unused land	31.16	57.03	334.89	9.11	19.48	46,284.82

Table A3. *Cont.*

Year	Land Use Type	Grassland	Building Site	Arable Land	Woodland	Body of Water	Unused Land
2005–2010	Grassland	35,875.75	305.95	4028.51	858.70	267.73	11,098.78
	Building land	106.08	1012.95	342.89	4.80	19.61	133.81
	Cropland	1099.33	428.33	13,760.99	29.27	49.44	75.76
	Forest land	2460.05	37.85	435.86	1722.13	27.08	214.13
	Water	641.23	12.26	44.30	0.82	1113.66	1464.82
	Unused land	6999.42	299.33	1384.45	24.70	302.14	37,541.26
2010–2015	Grassland	46,092.34	242.00	726.72	50.59	32.55	31.97
	Building land	2.02	2081.55	12.05	0.09	0.12	0.84
	Cropland	290.89	120.53	19,576.30	0.69	2.52	6.08
	Forest land	58.90	0.09	0.65	2580.20	0.18	0.41
	Water	54.65	50.27	2.79	0.24	1596.20	75.36
	Unused land	40.49	72.07	26.83	0.37	23.75	50,364.09
2015–2020	Grassland	43,457.96	343.31	1363.77	178.54	62.99	1129.79
	Building land	150.09	2205.39	69.29	0.23	4.44	137.06
	Cropland	406.44	273.82	19,624.12	4.72	9.71	26.49
	Forest land	284.35	7.34	9.72	2329.06	0.66	0.92
	Water	33.84	7.11	15.69	0.66	1529.74	67.76
	Unused land	3965.98	153.30	96.43	1.27	78.57	46,177.55

Table A4. Land use/cover classification of the northern slopes of the Tianshan Mountains.

Level I Land Category		Level II Land Category	
Grade	**Typology**	**Grade**	**Typology**
1	arable land	11	Paddy field
		12	Dryland
2	woodland	21	Forested land
		22	Shrubland
		23	Open woodland
		24	Other woodlands
3	grassland	31	High-cover grassland
		32	Medium-cover grassland
		33	Low cover grassland
4	body of water	41	Rivers and canals
		42	Lakes
		43	Reservoir pit ponds
		44	Permanent glacial snowfields
		46	Mudflats
5	urban, rural, industrial, mining, and residential land	51	Townsite
		52	Rural settlements
		53	Other building land
6	unused land	61	Sandy land
		62	Gobi
		63	Salt and alkaline land
		64	Marshland
		65	Bare land
		66	Bare rocky ground
		67	Other

References

1. Muhammed, K. *Modeling the Impact of Land Use on Habitat Quality in the Choctawhatchee River and Bay Watershed*; Florida Agricultural and Mechanical University: Tallahassee, FL, USA, 2022.
2. Pettorelli, N.; Gaillard, J.M.; Van Laere, G.; Duncan, P.; Kjellander, P.; Liberg, O.; Delorme, D.; Maillard, D. Variations in adult body mass in roe deer: The effects of population density at birth and of habitat quality. *Proc. R. Soc. B-Biol. Sci.* **2002**, *269*, 747–753. [CrossRef] [PubMed]
3. Mori, J.; Brown, W.; Skinner, D.; Schlichting, P.; Novakofski, J.; Mateus-Pinilla, N. An Updated Framework for Modeling White-Tailed Deer (*Odocoileus virginianus*) Habitat Quality in Illinois, USA. *Ecol. Evol.* **2024**, *14*, e70487. [CrossRef] [PubMed]
4. Wang, Y.; Xia, J.; Cai, W.; Liu, Z.; Li, J.; Yin, J.; Zu, J.; Dou, C. Response of Fish Habitat Quality to Weir Distribution Change in Mountainous River Based on the Two-Dimensional Habitat Suitability Model. *Sustainability* **2023**, *15*, 8698. [CrossRef]
5. DuBose, T.P.; Boor, G.K.H.; Fields, M.; Kalies, E.L.; Castillo, A.; Moskwik, M.P.; Marcus, J.F.; Walters, J.R. Remotely sensed habitat quality index reliably predicts an umbrella species presence but not demographic performance: A case study with open pine forests and red-cockaded woodpeckers. *Ecol. Indic.* **2023**, *154*, 110480. [CrossRef]
6. van Riper, C.J.; Kyle, G.T.; Sherrouse, B.C.; Bagstad, K.J.; Sutton, S.G. Toward an integrated understanding of perceived biodiversity values and environmental conditions in a national park. *Ecol. Indic.* **2017**, *72*, 278–287. [CrossRef]
7. van Riper, C.J.; Kyle, G.T.; Sutton, S.G.; Barnes, M.; Sherrouse, B.C. Mapping outdoor recreationists' perceived social values for ecosystem services at Hinchinbrook Island National Park, Australia. *Appl. Geogr.* **2012**, *35*, 164–173. [CrossRef]
8. Mondal, I.; Naskar, P.K.; Alsulamy, S.; Jose, F.; Hossain, S.K.A.; Mohammad, L.; De, T.K.; Khedher, K.M.; Salem, M.A.; Benzougagh, B.; et al. Habitat quality and degradation change analysis for the Sundarbans mangrove forest using invest habitat quality model and machine learning. *Environ. Dev. Sustain.* **2024**. [CrossRef]
9. Jiang, F.; Liu, C.; Zhao, J.; Jiang, B.; Fan, F. Habitat quality assessment on the Qinghai-Tibet plateau across vegetation ecoregions using InVEST and Geodetector models. *Front. Earth Sci.* **2024**, *12*, 1432434. [CrossRef]
10. Li, S.; Hong, Z.; Xue, X.; Zheng, X.; Du, S.; Liu, X. Evolution characteristics and multi-scenario prediction of habitat quality in Yulin City based on PLUS and InVEST models. *Sci. Rep.* **2024**, *14*, 11852. [CrossRef]
11. Jeong, A.; Kim, M.; Lee, S. Analysis of Priority Conservation Areas Using Habitat Quality Models and MaxEnt Models. *Animals* **2024**, *14*, 1680. [CrossRef]
12. Cheng, J.; Guo, F.; Wang, L.; Li, Z.; Zhou, C.; Wang, H.; Liang, W.; Jiang, X.; Chen, Y.; Dong, P. Evaluating the impact of ecological factors on the quality and habitat distribution of *Lonicera japonica* Flos using HPLC and the MaxEnt model. *Front. Plant Sci.* **2024**, *15*, 1397939. [CrossRef] [PubMed]
13. Bagstad, K.J.; Villa, F.; Batker, D.; Harrison-Cox, J.; Voigt, B.; Johnson, G.W. From theoretical to actual ecosystem services: Mapping beneficiaries and spatial flows in ecosystem service assessments. *Ecol. Soc.* **2014**, *19*, 64. [CrossRef]
14. Sherrouse, B.C.; Semmens, D.J.; Clement, J.M. An application of Social Values for Ecosystem Services (SolVES) to three national forests in Colorado and Wyoming. *Ecol. Indic.* **2014**, *36*, 68–79. [CrossRef]
15. Ma, Q.; Liu, K.; Gao, Y.; Li, Y.; Fan, Y.N.; Gu, C. Assessment on Social Values of Ecosystem Services in Xi'an Chanba National Wetland Park based on SolVES Model. *Wetl. Sci.* **2018**, *16*, 51–58. (In Chinese)
16. Vollering, J.; Halvorsen, R.; Mazzoni, S. The MIAmaxent R package: Variable transformation and model selection for species distribution models. *Ecol. Evol.* **2019**, *9*, 12051–12068. [CrossRef]
17. Yang, N.; Ma, D.Y.; Zhong, X.; Yang, K.; Zhou, Z.Q.; Zhou, H.L.; Zhou, C.Q.; Wang, B. Habitat suitability assessment of Blue Eared-Pheasant based on MaxEnt modeling in Wanglang National Nature Reserve, Sichuan Province. *Acta Ecol. Sin.* **2020**, *40*, 7064–7072. (In Chinese)
18. Vigerstol, K.L.; Aukema, J.E. A comparison of tools for modeling freshwater ecosystem services. *J. Environ. Manag.* **2011**, *92*, 2403–2409. [CrossRef]
19. Polasky, S.; Nelson, E.; Pennington, D.; Johnson, K.A. The Impact of Land-Use Change on Ecosystem Services, Biodiversity and Returns to Landowners: A Case Study in the State of Minnesota. *Environ. Resour. Econ.* **2011**, *48*, 219–242. [CrossRef]
20. Sanchez-Canales, M.; Lopez Benito, A.; Passuello, A.; Terrado, M.; Ziv, G.; Acuna, V.; Schuhmacher, M.; Javier Elorza, F. Sensitivity analysis of ecosystem service valuation in a Mediterranean watershed. *Sci. Total Environ.* **2012**, *440*, 140–153. [CrossRef]
21. Aneseyee, A.B.; Noszczyk, T.; Soromessa, T.; Elias, E. The InVEST Habitat Quality Model Associated with Land Use/Cover Changes: A Qualitative Case Study of the Winike Watershed in the Omo-Gibe Basin, Southwest Ethiopia. *Remote Sens.* **2020**, *12*, 1103. [CrossRef]
22. He, B.; Chang, J.; Guo, A.; Wang, Y.; Wang, Y.; Li, Z. Assessment of river basin habitat quality and its relationship with disturbance factors: A case study of the Tarim River Basin in Northwest China. *J. Arid Land* **2022**, *14*, 167–185. [CrossRef]
23. Chen, C.; Liu, J.; Bi, L. Spatial and Temporal Changes of Habitat Quality and Its Influential Factors in China Based on the InVEST Model. *Forests* **2023**, *14*, 374. [CrossRef]
24. Kim, T.; Song, C.; Lee, W.-K.; Kim, M.; Lim, C.-H.; Jeon, S.W.; Kim, J. Habitat Quality Valuation Using InVEST Model in Jeju Island. *J. Korea Soc. Environ. Restor. Technol.* **2015**, *18*, 1–11. [CrossRef]

25. Leh, M.D.K.; Matlock, M.D.; Cummings, E.C.; Nalley, L.L. Quantifying and mapping multiple ecosystem services change in West Africa. *Agric. Ecosyst. Environ.* **2013**, *165*, 6–18. [CrossRef]
26. Zhang, X.; Song, W.; Lang, Y.; Feng, X.; Yuan, Q.; Wang, J. Land use changes in the coastal zone of China's Hebei Province and the corresponding impacts on habitat quality. *Land Use Policy* **2020**, *99*, 104957. [CrossRef]
27. Pu, J.; Shen, A.; Liu, C.; Wen, B. Impacts of ecological land fragmentation on habitat quality in the Taihu Lake basin in Jiangsu Province, China. *Ecol. Indic.* **2024**, *158*, 111611. [CrossRef]
28. Ding, Q.; Chen, Y.; Bu, L.; Ye, Y. Multi-Scenario Analysis of Habitat Quality in the Yellow River Delta by Coupling FLUS with InVEST Model. *Int. J. Environ. Res. Public Health* **2021**, *18*, 2389. [CrossRef]
29. Kim, H.N.; Ryu, H. Estimating the Economic Value of Change in Ecosystem Habitat Quality in South Korea Using an Integrated Environmental and Economic Analysis. *Land* **2022**, *11*, 2249. [CrossRef]
30. Yang, J.; Xie, B.; Zhang, D. Spatial-temporal evolution of habitat quality and its influencing factors in the Yellow River Basin based on InVEST model and GeoDetector. *J. Desert Res.* **2021**, *41*, 12.
31. Tang, F.; Fu, M.; Wang, L.; Song, W.; Yu, J.; Wu, Y. Dynamic evolution and scenario simulation of habitat quality under the impact of land-use change in the Huaihe River Economic Belt, China. *PLoS ONE* **2021**, *16*, e0249566. [CrossRef]
32. Tang, F.; Fu, M.; Wang, L.; Zhang, P. Land-use change in Changli County, China: Predicting its spatio-temporal evolution in habitat quality. *Ecol. Indic.* **2020**, *117*, 106719. [CrossRef]
33. Upadhaya, S.; Dwivedi, P. Conversion of of forestlands to blueberries: Assessing implications for habitat quality in Alabaha river watershed in Southeastern Georgia, United States. *Land Use Policy* **2019**, *89*, 104229. [CrossRef]
34. Sun, X.; Jiang, Z.; Liu, F.; Zhang, D. Monitoring spatio-temporal dynamics of habitat quality in Nansihu Lake basin, eastern China, from 1980 to 2015. *Ecol. Indic.* **2019**, *102*, 716–723. [CrossRef]
35. Chen, M.; Bai, Z.; Wang, Q.; Shi, Z. Habitat Quality Effect and Driving Mechanism of Land Use Transitions: A Case Study of Henan Water Source Area of the Middle Route of the South-to-North Water Transfer Project. *Land* **2021**, *10*, 796. [CrossRef]
36. Tian, F.; Liu, L.-Z.; Yang, J.-H.; Wu, J.-J. Vegetation greening in more than 94% of the Yellow River Basin (YRB) region in China during the 21st century caused jointly by warming and anthropogenic activities. *Ecol. Indic.* **2021**, *125*, 107479. [CrossRef]
37. Xu, L.; Du, H.; Zhang, X. Driving forces of carbon dioxide emissions in China's cities: An empirical analysis based on the geodetector method. *J. Clean. Prod.* **2021**, *287*, 125169. [CrossRef]
38. Zhu, H.; Wang, J.; Tang, J.; Ding, Z.; Gong, L. Spatiotemporal variations of ecosystem services and driving factors in the Tianchi Bogda Peak Natural Reserve of Xinjiang, China. *J. Arid Land* **2024**, *16*, 816–833. [CrossRef]
39. Li, H.; Cui, S.; Zhao, C.; Zhang, H. Assessing Trade-Offs and Synergies in Ecosystem Services within the Tianshan Mountainous Region. *Water* **2024**, *16*, 2921. [CrossRef]
40. Kou, Y.; Chen, S.; Zhou, K.; Qiu, Z.; He, J.; Shi, X.; Zhou, X.; Zhang, Q. Spatiotemporal Patterns and Coupling Coordination Analysis of Multiscale Social-Economic-Ecological Effects in Ecologically Vulnerable Areas Based on Multi-Source Data: A Case Study of the Tuha Region, Xinjiang Province. *Land* **2024**, *13*, 282. [CrossRef]
41. Wei, Y.; Wang, H.; Xue, M.; Yin, Y.; Qian, T.; Yu, F. Spatial and Temporal Evolution of Land Use and the Response of Habitat Quality in Wusu, China. *Int. J. Environ. Res. Public Health* **2023**, *20*, 361. [CrossRef]
42. Lu, Y.; Zhao, J.; Qi, J.; Rong, T.; Wang, Z.; Yang, Z.; Han, F. Monitoring the Spatiotemporal Dynamics of Habitat Quality and Its Driving Factors Based on the Coupled NDVI-InVEST Model: A Case Study from the Tianshan Mountains in Xinjiang, China. *Land* **2022**, *11*, 1805. [CrossRef]
43. Han, C.; Zheng, J.; Han, W.; Lu, B.; Yu, W.; Wang, Z.; Yang, J.; Wu, J. Research on habitat quality in arid urban agglomerations: Influencing mechanisms and multi-scenario simulations. *Land Degrad. Dev.* **2024**, *35*, 2256–2273. [CrossRef]
44. Wang, H.Z.; Li, R.D.; Wu, H.H. Bilateral change dynamic degree model for land use and its application to the land use study of in suburban areas of wuhan. *Remote Sens. Land Resour.* **2002**, *14*, 20–22. (In Chinese)
45. Liu, D.; Li, L.N. Spatiotemporal change and driving factors of land use in the northern border transect of China. *Resour. Sci.* **2021**, *43*, 1208–1221. (In Chinese)
46. Liu, M.Y. Assessment of Carbon Storage and Habitat Quality in Hexi Region Based on InVEST Model. Master's Thesis, Lanzhou University, Lanzhou, China, 2023. (In Chinese)
47. Wang, Y.; Gao, J.X.; Jin, Y.; Cao, B.S.; Wang, Y.; Zhang, X.H.; Zhou, J.W. Habitat Quality of Farming-pastoral Ecotone in Bairin Right Banner, Inner Mongolia Based on Land Use Change and InVEST Model From 2005 to 2015. *J. Ecol. Rural Environ.* **2020**, *36*, 654–662. (In Chinese) [CrossRef]
48. Xie, Y.F.; Yao, S.B.; Deng, Y.J.; Jia, L.; LI, Y.Y.; Gao, Q. Impact of the 'Grain for Green' project on the spatial and temporal. *Chin. J. Eco-Agric.* **2020**, *28*, 575–586. (In Chinese) [CrossRef]
49. Chen, Y.; Qiao, F.; Jiang, L. Effects of Land Use Pattern Change on Regional Scale Habitat Quality Based on InVEST Model—A Case Study in Beijing. *Acta Sci. Nat. Univ. Pekin.* **2016**, *52*, 553–562. (In Chinese) [CrossRef]

50. Reheman, R.; Kasim, A.; Ablat, H.; Duolat, X.; Xu, J.H. Research on the Temporal and Spatial Evolution of Habitat Quality in Urban Agglomeration on the Northern Slope of Tianshan Mountains Based on InVEST Model. *J. Ecol. Rural Environ.* **2022**, *38*, 1112–1121. (In Chinese) [CrossRef]
51. Liu, F.T.; Xu, E.Q. Comparison of spatial-temporal evolution of habitat quality between Xinjiang Corps and Non-corps Region based on land use. *Chin. J. Appl. Ecol.* **2020**, *31*, 2341–2351. (In Chinese) [CrossRef]
52. Lu, M.; Wang, H.S.; Xun, X. Spatial-temporal evolution of habitat quality in Altay area and its driving factors. *J. Beijing For. Univ.* **2024**, *46*, 27–39. (In Chinese)
53. Xiao, H.Y. Research on the Spatiotemporal Evolution of Habitat Quality in Guiyang City Based on Land Use Change. Master's Thesis, Guizhou University, Guiyang, China, 2022. (In Chinese)
54. Zhang, S.; Han, L.; Cao, H.Y. Habitat quality assessment of the Weihe Basin based on the InVEST model. *J. Lanzhou Univ. (Nat. Sci.)* **2024**, *60*, 159–166+172. (In Chinese) [CrossRef]
55. Ai, J.H. Analysis on Spatial and Temporal Evolution of Habitat Quality in the Koshi River Basin Based on the Land Use /Cover Change. Master's Thesis, Jiangxi Normal University, Nanchang, China, 2021. (In Chinese)
56. Moran, P.A.P. Notes on continuous stochastic phenomena. *Biometrika* **1950**, *37*, 17–23. [CrossRef] [PubMed]
57. Chen, S.; Liu, X. Spatio-temporal variations of habitat quality and its driving factors in the Yangtze River Delta region of China. *Glob. Ecol. Conserv.* **2024**, *52*, e02978. [CrossRef]
58. Li, T.; Bao, R.; Li, L.; Tang, M.; Deng, H. Temporal and Spatial Changes of Habitat Quality and Their Potential Driving Factors in Southwest China. *Land* **2023**, *12*, 346. [CrossRef]
59. Qi, Y.; Hu, Y. Spatiotemporal Variation and Driving Factors Analysis of Habitat Quality: A Case Study in Harbin, China. *Land* **2024**, *13*, 67. [CrossRef]
60. Zhang, H.; Wang, F.; Zhao, H.; Kang, P.; Tang, L. Evolution of habitat quality and analysis of influencing factors in the Yellow River Delta Wetland from 1986 to 2020. *Front. Ecol. Evol.* **2022**, *10*, 1075914. [CrossRef]
61. Dong, B.W.; Huang, T.T.; Tang, T.; Huang, D.L.; Tang, C. Impact of multi-scenario land-use changes on habitat quality evolution in the Yangtze River economic belt. *Front. Environ. Sci.* **2025**, *12*, 1516703. [CrossRef]
62. Zhang, W.; Lu, X.D.; Xie, Z.X.; Ma, J.J.; Zang, J.M. Study on the Spatiotemporal Evolution of Habitat Quality in Highly Urbanized Areas Based on Bayesian Networks: A Case Study from Shenzhen, China. *Sustainability* **2024**, *16*, 10993. [CrossRef]
63. Kang, J.M.; Yang, F.S.; Wang, J.; Liu, Y.; Fang, D.M.; Jiang, C.C. Spatial-temporal evolution of habitat quality in tropical monsoon climate region based on "pattern-process-quality"—A case study of Cambodia. *Open Geosci.* **2025**, *17*, 20220748. [CrossRef]
64. Di Febbraro, M.; Sallustio, L.; Vizzarri, M.; De Rosa, D.; De Lisio, L.; Loy, A.; Eichelberger, B.A.; Marchetti, M. Expert-based and correlative models to map habitat quality: Which gives better support to conservation planning? *Glob. Ecol. Conserv.* **2018**, *16*, e00513. [CrossRef]
65. Louis, V.; Page, S.E.; Tansey, K.J.; Jones, L.; Bika, K.; Balzter, H. Tiger Habitat Quality Modelling in Malaysia with Sentinel-2 and InVEST. *Remote Sens.* **2024**, *16*, 284. [CrossRef]